

Functionalization of Acetylene-Terminated Monolayers on Si(100) Surfaces: A Click Chemistry Approach

Simone Ciampi,[†] Till Böcking,[†] Kristopher A. Kilian,[†] Michael James,[‡]
Jason B. Harper,[†] and J. Justin Gooding^{*,†}

School of Chemistry, The University of New South Wales, Sydney, NSW 2052 Australia, and The Bragg Institute, Australian Nuclear Science and Technology Organisation (ANSTO), Lucas Heights Research Laboratory, Lucas Heights, NSW 2234, Australia

Received April 10, 2007. In Final Form: May 30, 2007

In this article, we report the functionalization of alkyne-terminated alkyl monolayers on Si(100) using “click” chemistry, specifically, the Cu(I)-catalyzed Huisgen 1,3-dipolar cycloaddition reaction of azides with surface-bound alkynes. Covalently immobilized, structurally well-defined acetylene-terminated organic monolayers were prepared from a commercially available terminal diyne species using a one-step hydrosilylation procedure. Subsequent derivatization of the alkyne-terminated monolayers in aqueous environments with representative azide species via a selective, reliable, robust cycloaddition process afforded disubstituted surface-bound [1,2,3]-triazole species. Neither activation procedures nor protection/deprotection steps were required, as is the case with more established grafting approaches for silicon surfaces. Detailed characterization using X-ray photoelectron spectroscopy and X-ray reflectometry demonstrated that the surface acetylenes had reacted in moderate to high yield to give surfaces exposing alkyl chains, oligoether anti-fouling moieties, and functionalized aromatic structures. These results demonstrate that click immobilization offers a versatile, experimentally simple, chemically unambiguous modular approach to producing modified silicon surfaces with organic functionality for applications as diverse as biosensors and molecular electronics.

Introduction

The production of self-assembled monolayers (SAMs) has opened routes to the fabrication of assemblies onto surfaces with something akin to molecular-level control.^{1–3} This selective control of surface chemistry enables multiple components to be incorporated within a single monolayer as well as allowing SAMs to be subsequently used as platforms to which further molecular or nanoscale components can be attached with controlled surface density. Further derivatization of the SAM once it is formed, the so-called stepwise strategy, is a very popular method for the fabrication of complex, chemically heterogeneous molecular assemblies onto a surface.^{4–8} The popularity of this modular approach is related to both the versatility and ease of building up assemblies using this strategy. The versatility arises because components that are incompatible under the conditions of SAM formation can subsequently be attached to the surface under conditions in which they are stable.^{9–12} In particular, this is

important in integrating biological molecules with a surface.^{1,13–16} The ease of building assemblies using the stepwise strategy is due to the fact that the majority of the basic molecular components are commercially available and can be attached to the surface using straightforward, well-described coupling techniques.^{17–21} The major drawback of this derivatization approach is its intrinsic dependence on the efficiency and reliability of the particular coupling approach used and any eventual protection/deprotection steps involved. Coupling reactions involving immobilized molecular components typically display yields below 50% with the resulting presence of unreacted starting material and eventual side products posing serious limitations when molecular assembly with well-defined properties is pursued.^{22–24} An alternative strategy is to custom synthesize all of the different components prior to the assembly process. The advantage of this strategy is

* To whom correspondence should be addressed. E-mail: justin.gooding@unsw.edu.au.

[†] The University of New South Wales.

[‡] Australian Nuclear Science and Technology Organisation (ANSTO).

(1) Gooding, J. J.; Mearns, F.; Yang, W.; Liu, J. *Electroanalysis* **2003**, *15*, 81–96.

(2) Love, J. C.; Estroff, L. A.; Kriebel, J. K.; Nuzzo, R. G.; Whitesides, G. M. *Chem. Rev.* **2005**, *105*, 1103–1169.

(3) Wayner, D. D. M.; Wolkow, R. A. *J. Chem. Soc., Perkin Trans. 2* **2002**, 23–34.

(4) Strother, T.; Cai, W.; Zhao, X.; Hamers, R. J.; Smith, L. M. *J. Am. Chem. Soc.* **2000**, *122*, 1205–1209.

(5) Böcking, T.; James, M.; Coster, H. G. L.; Chilcott, T. C.; Barrow, K. D. *Langmuir* **2004**, *20*, 9227–9235.

(6) Böcking, T.; Kilian, K. A.; Gaus, K.; Gooding, J. J. *Langmuir* **2006**, *22*, 3494–3496.

(7) Böcking, T.; Wong, E. L. S.; James, M.; Watson, J. A.; Brown, C. L.; Chilcott, T. C.; Barrow, K. D.; Coster, H. G. L. *Thin Solid Films* **2006**, *515*, 1857–1863.

(8) Dutta, S.; Perring, M.; Barret, S.; Mitchell, M.; Kenis, P. J. A.; Bowden, N. B. *Langmuir* **2006**, *22*, 2146–2155.

(9) Sieval, A. B.; Demirel, A. L.; Nissink, J. W. M.; Linford, M. R.; van der Maas, J. H.; de Jeu, W. H.; Zuilhof, H.; Sudhölter, E. J. R. *Langmuir* **1998**, *14*, 1759–1768.

(10) Yan, L.; Huck, W. T. S.; Zhao, X.-M.; Whitesides, G. M. *Langmuir* **1999**, *15*, 1208–1214.

(11) Sieval, A. B.; Linke, R.; Heij, G.; Meijer, G.; Zuilhof, H.; Sudhölter, E. J. R. *Langmuir* **2001**, *17*, 7554–7559.

(12) Perring, M.; Dutta, S.; Arafat, S.; Mitchell, M.; Kenis, P. J. A.; Bowden, N. B. *Langmuir* **2005**, *21*, 10537–10544.

(13) Gooding, J. J.; Hibbert, D. B. *TrAC, Trends Anal. Chem.* **1999**, *18*, 525–533.

(14) Lin, Z.; Strother, T.; Cai, W.; Cao, X.; Smith, L. M.; Hamers, R. J. *Langmuir* **2002**, *18*, 788–796.

(15) Böcking, T.; Kilian, K. A.; Hanley, T.; Ilyas, S.; Gaus, K.; Gal, M.; Gooding, J. J. *Langmuir* **2005**, *21*, 10522–10529.

(16) Coffinier, Y.; Olivier, C.; Perzyna, A.; Grandidier, B.; Wallart, X.; Durand, J.-O.; Melnyk, O.; Stiévenard, D. *Langmuir* **2005**, *21*, 1489–1496.

(17) Janolino, V. G.; Swaisgood, H. E. *Biotechnol. Bioeng.* **1982**, *24*, 1069–1080.

(18) Boukherroub, R.; Wayner, D. D. M. *J. Am. Chem. Soc.* **1999**, *121*, 11513–11515.

(19) Strother, T.; Hamers, R. J.; Smith, L. M. *Nucleic Acids Res.* **2000**, *28*, 3535–3541.

(20) Boukherroub, R.; Wojtyk, J. T. C.; Wayner, D. D. M.; Lockwood, D. J. *J. Electrochem. Soc.* **2002**, *149*, H59–H63.

(21) Voicu, R.; Boukherroub, R.; Bartzoka, V.; Ward, T.; Wojtyk, J. T. C.; Wayner, D. D. M. *Langmuir* **2004**, *20*, 11713–11720.

(22) Jiang, L.; Glidle, A.; Griffith, A.; McNeil, C. J.; Cooper, J. M. *Bioelectrochemistry* **1997**, *42*, 15–23.

(23) Liu, J.; Paddon-Row, M. N.; Gooding, J. J. *J. Phys. Chem. B* **2004**, *108*, 8460–8466.

that purified components can be attached to the surface. However, the disadvantages are that the strategy is less versatile, more synthetically demanding, and if components in the monolayer-forming molecules have footprints larger than the distance between close-packed molecules in the monolayer, a defect-free monolayer will not be produced.^{9,18}

Achieving the best of both of these strategies requires coupling chemistry that provides quantitative coupling of additional components to surfaces. Such a requirement can be met only when coupling reactions are driven by favorable thermodynamics (thus giving high yields), are selective enough to tolerate functional groups present in the reaction environment, and are not significantly hampered by steric factors. A recent publication by Chidsey and co-workers seems to indicate that such surface chemistry has been found.²⁵ In this work, FTIR spectroscopy evidence for quantitative coupling of ferrocene molecules to the surface of a SAM formed on a gold electrode is produced. The coupling process used was a variant of the Huisgen 1,3-dipolar cycloaddition reaction of a SAM with terminal azide groups to an alkyne in solution.^{26–27}

The Huisgen 1,3-dipolar cycloaddition is one of several fusion processes recently designated as a “click” reaction by Sharpless and colleagues.²⁸ An ideal click reaction should be of a wide scope, be selective, be high yielding, require minimum purification effort (if any), and be generally insensitive to the most common reaction parameters (solvent, temperature, molecular oxygen). Within this class of transformations, the coupling of azides to terminal alkynes, to yield disubstituted [1,2,3]-triazoles, through a Cu(I)-catalyzed version of the Huisgen 1,3-dipolar cycloaddition reaction has been shown to be arguably the most useful reaction.²⁹ The presence of a copper(I) catalyst results in regioselective, high-yielding cycloaddition processes that reach completion at short reaction times under mild and experimentally simple conditions.^{30–34} The click chemistry of azides and acetylenes has recently been successfully applied to solution-phase chemistry,^{30,35–41} to in vivo and in vitro bioconjugation

strategies,^{42–44} and, more recently, to the field of surface chemistry, with examples including modifications of gold electrodes,^{25,45–48} glass surfaces,⁴⁹ silicon oxide,^{50–52} silicon(111),⁵³ and metal microparticles.^{54–56}

Our primary research interest is in the organic and biomolecular modification of flat, nanoporous silicon for biosensing^{57–59} and molecular electronics.^{60–62} We are interested in silicon because of the compatibility of silicon with bulk manufacturing and with developing photonic structures.^{63,64} Hydrosilylation of unsaturated hydrocarbons represents the method of choice when environmentally robust, chemically unambiguous, ordered monolayers on silicon are required.^{3,65,66} However, we have shown how any disruption in the packing of the monolayer-forming molecules may lead to oxidation of the underlying substrate with even barely detectable amounts of silicon oxide species impairing the electronic⁶² and optical properties⁵⁷ of the hybrid organic–silicon assembly. Virtually oxide-free surfaces can be prepared when covalent grafting at the silicon substrate of functionalized alkene molecules is followed by the attachment of additional components in a stepwise manner.⁵⁷ Conversely, when analogous surfaces are prepared via grafting of a preassembled, complex, organic molecules, inferior surface coverages are achieved, and increased levels of silicon oxide species detected.⁶ Thus, there is a definite need for efficient stepwise assembly strategies applicable to silicon surfaces. The only published work that focused on click chemistry applied to silicon surfaces is by Rohde et al., where a fully

(24) Non-quantitative yields for eventual protection/activation procedures pose limitations when high-quality surface modification is pursued. The presence of unreacted *N*-hydroxysuccinimide esters, upon reaction with an intended nucleophile, is a general example (Liu, G.; Nguyen, Q. T.; Chow, E.; Böcking, T.; Hibbert, D. B.; Gooding, J. J. *Electroanalysis* **2006**, *18*, 1141–1151).

(25) Collman, J. P.; Devaraj, N. K.; Chidsey, C. E. D. *Langmuir* **2004**, *20*, 1051–1053.

(26) Huisgen, R. *Pure Appl. Chem.* **1989**, *61*, 613–628.

(27) Huisgen, R. *1,3-Dipolar Cycloaddition Chemistry*; Wiley: New York, 1984.

(28) Kolb, H. C.; Finn, M. G.; Sharpless, K. B. *Angew. Chem., Int. Ed.* **2001**, *40*, 2004–2021.

(29) Kolb, H. C.; Sharpless, K. B. *Drug Discovery Today* **2003**, *8*, 1128–1137.

(30) Rostovstev, V. V.; Green, L. G.; Fokin, V. V.; Sharpless, K. B. *Angew. Chem., Int. Ed.* **2002**, *41*, 2596–2599.

(31) Tornøe, C. W.; Christensen, C.; Meldal, M. *J. Org. Chem.* **2002**, *67*, 3057–3064.

(32) Wang, Q.; Chan, T. R.; Hilgraf, R.; Fokin, V. V.; Sharpless, K. B.; Finn, M. G. *J. Am. Chem. Soc.* **2003**, *125*, 3192–3193.

(33) Wu, P.; Feldman, A. K.; Nugent, A. K.; Hawker, C. J.; Scheel, A.; Voit, B.; Pyun, J.; Fréchet, J. M. J.; Sharpless, K. B.; Fokin, V. V. *Angew. Chem., Int. Ed.* **2004**, *43*, 3928–3932.

(34) Bock, V. D.; Hiemstra, H.; van Maarseveen, J. H. *Eur. J. Org. Chem.* **2006**, 51–68.

(35) Wang, J.; Sui, G.; Mocharla, V. P.; Lin, R. J.; Phelps, M. E.; Kolb, H. C.; Tseng, H.-R. *Angew. Chem., Int. Ed.* **2006**, *45*, 5276–5281.

(36) Ornelas, C.; Aranzas, J. R.; Cloutet, E.; Alves, S.; Astruc, D. *Angew. Chem., Int. Ed.* **2007**, *46*, 872–877.

(37) Thibault, R. J.; Takizawa, K.; Lowenheilm, P.; Helms, B.; Mynar, J. L.; Fréchet, J. M. J.; Hawker, C. J. *J. Am. Chem. Soc.* **2006**, *128*, 12084–12085.

(38) Chittaboina, S.; Xie, F.; Wang, Q. *Tetrahedron Lett.* **2005**, *46*, 2331–2336.

(39) Taylor, M. S.; Zalatan, D. N.; Lerchner, A. M.; Jacobsen, E. N. *J. Am. Chem. Soc.* **2005**, *127*, 1313–1317.

(40) Fernandez-Megia, E.; Correa, J.; Riguera, R. *Biomacromolecules* **2006**, *7*, 3104–3111.

(41) Ryu, E.-H.; Zhao, Y. *Org. Lett.* **2005**, *7*, 1035–1037.

(42) Speers, A. E.; Cravatt, B. F. *Chem. Biol.* **2004**, *11*, 535–546.

(43) Speers, A. E.; Adam, G. C.; Cravatt, B. F. *J. Am. Chem. Soc.* **2003**, *125*, 4686–4687.

(44) Link, A. J.; Tirrell, D. A. *J. Am. Chem. Soc.* **2003**, *125*, 11164–11165.

(45) Lee, J. K.; Chi, Y. S.; Choi, I. S. *Langmuir* **2004**, *20*, 3844–3847.

(46) Devaraj, N. K.; Decreau, R. A.; Ebina, W.; Collman, J. P.; Chidsey, C. E. D. *J. Phys. Chem. B* **2006**, *110*, 15955–15962.

(47) Zhang, Y.; Luo, S.; Tang, Y.; Yu, L.; Hou, K.-Y.; Cheng, J.-P.; Zeng, X.; Wang, P. G. *Anal. Chem.* **2006**, *78*, 2001–2008.

(48) Collman, J. P.; Devaraj, N. K.; Eberspacher, T. P. A.; Chidsey, C. E. D. *Langmuir* **2006**, *22*, 2457–2464.

(49) Sun, X.-L.; Stabler, C. L.; Cazalis, C. S.; Chaikof, E. L. *Bioconjugate Chem.* **2006**, *17*, 52–57.

(50) Rozkiewicz, D. I.; Janczewski, D.; Verboom, W.; Ravoo, B. J.; Reinhoudt, D. N. *Angew. Chem., Int. Ed.* **2006**, *45*, 5292–5296.

(51) Lummerstorfer, T.; Hoffmann, H. *J. Phys. Chem. B* **2004**, *108*, 3963–3966.

(52) Kacprzak, K. M.; Maier, N. M.; Lindner, W. *Tetrahedron Lett.* **2006**, *47*, 8721–8726.

(53) Rohde, R. D.; Agnew, H. D.; Yeo, W.-S.; Bailey, R. C.; Heath, J. R. J. *Am. Chem. Soc.* **2006**, *128*, 9518–9525.

(54) White, M. A.; Johnson, J. A.; Koberstein, J. T.; Turro, N. J. *J. Am. Chem. Soc.* **2006**, *128*, 11356–11357.

(55) Brennan, J. L.; Hatzakis, N. S.; Tshikhudo, T. R.; Dirvianskyte, N.; Razumas, V.; Patkar, S.; Vind, J.; Svendsen, A.; Nolte, R. J. M.; Rowan, A. E.; Brust, M. *Bioconjugate Chem.* **2006**, *17*, 1373–1375.

(56) Fleming, D. A.; Thode, C. J.; Williams, M. E. *Chem. Mater.* **2006**, *18*, 2327–2334.

(57) Kilian, K. A.; Böcking, T.; Gaus, K.; Gal, M.; Gooding, J. J. *Biomaterials* **2007**, *28*, 3055–3062.

(58) Kilian, K. A.; Böcking, T.; Ilyas, S.; Jessup, W.; Gaus, K.; Gal, M.; Gooding, J. J. *Adv. Funct. Mater.*, in press.

(59) Kilian, K. A.; Böcking, T.; Gaus, K.; King-Lacroix, J.; Gal, M.; Gooding, J. J. *Chem. Commun.* **2007**, 1936–1938.

(60) Böcking, T.; Salomon, A.; Cahen, D.; Gooding, J. J. *Langmuir* **2007**, *23*, 3236–3241.

(61) Salomon, A.; Böcking, T.; Gooding, J. J.; Cahen, D. *Nano Lett.* **2006**, *6*, 2873–2876.

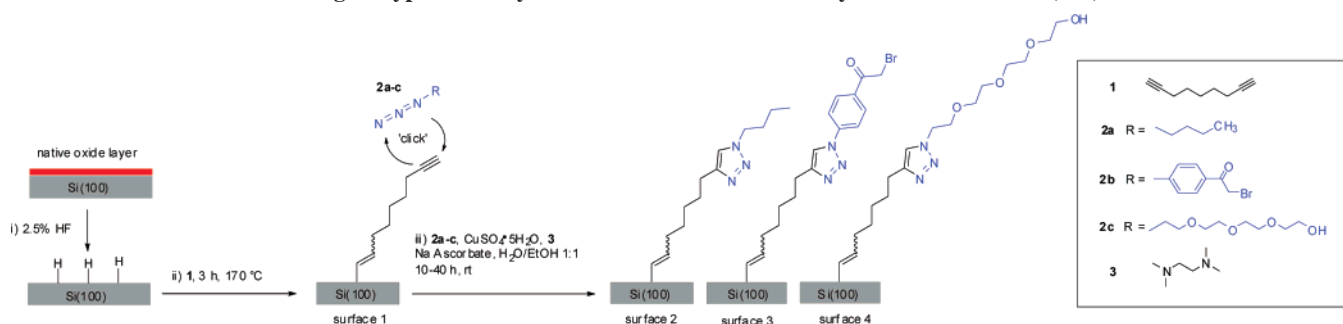
(62) Seitz, O.; Böcking, T.; Salomon, A.; Gooding, J. J.; Cahen, D. *Langmuir* **2006**, *22*, 6915–6922.

(63) Sailor, M. J.; Link, J. R. *Chem. Commun.* **2005**, *11*, 1375–1383.

(64) Ilyas, S.; Böcking, T.; Kilian, K. A.; Reece, P. J.; Gooding, J. J.; Gaus, K.; Gal, M. *Opt. Mater.* **2007**, *29*, 619–622.

(65) (a) Linford, M. R.; Chidsey, C. E. D. *J. Am. Chem. Soc.* **1993**, *115*, 12631–12632. (b) Linford, M. R.; Fenter, P.; Eisenberger, P. M.; Chidsey, C. E. D. *J. Am. Chem. Soc.* **1995**, *117*, 3145–3155. (c) Sung, M. M.; Kluth, G. J.; Yauw, O. W.; Maboudian, R. *Langmuir* **1997**, *13*, 6164–6168. (d) Cicero, R. L.; Linford, M. R.; Chidsey, C. E. D. *Langmuir* **2000**, *16*, 5688–5695. (e) Sieval, A. B.; Linke, R.; Zuilhof, H.; Sudhölter, E. J. R. *Adv. Mater.* **2000**, *12*, 1457–1460.

(66) For a comprehensive review on organometallic chemistry of silicon and germanium, see Buriak, J. M. *Chem. Rev.* **2002**, *102*, 1271–1308.

Scheme 1. Huisgen-Type Click Cycloaddition Reactions on Acetylene-Terminated Si(100) Surfaces^a

^a (i) Single-side-polished Si(100) wafers were immersed in aqueous 2.5% HF for 90 s to remove the native silicon dioxide layer. (ii) The resulting metastable, hydride-terminated surface was reacted with neat (terminal) diacetylene species **1** to afford the corresponding hydrosilylation product (surface 1). (iii) Covalently modified surface 1, favorably presenting an alkyne functionality, afforded a convenient dipolarophile in the preparation of surface-bound 1,4-disubstituted [1,2,3]-triazoles (entries 1–8, Table 1, surfaces 2–4) through Cu(I)-catalyzed click coupling reactions with differently substituted azides (**2a–2c**). The depiction of the silicon surface upon click reaction shows molecular components that are colored for clarity.

acetylene-terminated Si(111) surface is coupled, albeit in 7% yield, to a solution-phase substituted azide.⁵³ The observed poor outcome of the click step was reasoned to be a direct consequence of the significant steric hindrance introduced upon conversion of densely packed surface alkynes to the corresponding immobilized triazole species. However, this study was focused on full surface passivation, with every surface silicon atom site grafted to an sp-hybridized carbon atom, as distinct from an average of every second silicon surface atom as achieved on a Si(111) surface using hydrosilylation.^{5,65b} Hence no attempt was made to achieve better surface coverage.

The purpose of this article is to provide a detailed characterization of organic structures prepared via click chemistry on high-quality covalent monolayers on silicon surfaces. Our surface modification approach is outlined in Scheme 1. 1,8-Nonadiyne (**1**), the starting material used in the preparation of the acetylene-terminated surface, was chosen as a convenient candidate for the evaluation of the outcome of our synthesis strategy because it exhibits a number of key properties. Being commercially available, no synthesis effort was required for its preparation. Furthermore, its symmetrical nature allowed the intended alkyne-terminated monolayer to be prepared in a single-step procedure using hydrosilylation chemistry.⁶⁷ The preparation of an alkyne-terminated, covalently grafted organic monolayer was followed by a click reaction of the prepared surface-bound dipolarophile (the acetylene function) with representative substituted azides either in the presence or absence of the Cu(I)-stabilizing species *N,N,N',N'*-tetramethylethylenediamine (**3**).⁶⁸ All surfaces were characterized using contact angle goniometry, X-ray photoelectron spectroscopy (XPS), and X-ray reflectometry (XRR). Azido compounds **2a–2c** used in the click step were chosen to impart a range of physical, spectroscopic, and chemical properties to the modified silicon substrate. Compound **2a** was chosen to aid in spectroscopic characterization. Functionalities introduced by compound **2b** may allow, upon nucleophilic substitution of the bromine atom, further immobilization of thiols onto the modified

surface (surface 3). Finally, the tetra(ethylene glycol) moiety present in compound **2c** (and exposed by the corresponding triazole product, surface 4) was introduced to impart resistance toward nonspecific adsorption of protein,^{69–72} a fundamental prerequisite for a potential biorecognition interface.^{15,73}

Experimental Methods

Materials. Chemicals. All chemicals, unless otherwise noted, were of analytical grade and used as received. Chloroform, ethyl acetate, and ethanol for substrate cleaning were redistilled prior to use. Milli-Q water (~18 MΩ cm) was used to prepare solutions and for chemical reactions and surface cleaning. Hydrogen peroxide (30 wt % in water, Sigma-Aldrich), hydrofluoric acid (Riedel-de Haën, 48 wt % in water), and sulfuric acid (J. T. Baker) were either of semiconductor or analogous grade. 4-Azidophenacyl bromide **2b** (98% purity) was from Sigma-Aldrich. 1,8-Nonadiyne **1** (Aldrich) of a nominal purity of 98% was redistilled from sodium borohydride (Sigma-Aldrich, 99+% purity) under reduced pressure (79 °C, 8 to 9 Torr), collected over molecular sieves (4 Å) and stored under an argon atmosphere prior to use. Dichloromethane and pyridine, used as solvents in chemical reactions, were distilled from calcium hydride and potassium hydroxide, respectively, and stored over molecular sieves prior to use. *N,N*-Dimethylformamide (Fluka, 98+%) was distilled under reduced pressure from calcium hydride. *p*-Toluenesulfonyl chloride (Sigma-Aldrich, 98%) was recrystallized from chloroform (EMD Chemicals, HPLC grade)/hexane (redistilled). Sodium azide (Sigma-Aldrich) was crystallized from water by the addition of ethanol. Albumin-fluorescein isothiocyanate conjugate (FITC-BSA, ≥7 mol FITC per mol albumin) was purchased from Sigma.

Wafers. Single-side-polished silicon wafers (100-oriented, p-type, ~400 μm thick, 0.20–0.30 Ω cm resistivity) were obtained from Wacker-Chemitronic GMBH.

Purification and Analysis of Synthesized Compounds. Thin-layer chromatography (TLC) was performed on Merck silica gel aluminum sheets (60 F₂₅₄). Merck silica gel (grade 9385, 230–400 mesh) was used for column chromatography. NMR spectra were recorded on a Bruker Avance 300 spectrometer, using the solvent signal (CDCl₃ from Aldrich, passed through basic alumina) as an internal reference. FTIR spectra were recorded on a Thermo Nicolet Avatar 370 FTIR spectrometer by accumulating a minimum of 32

(67) For examples on the thermal, non-catalyzed hydrosilylation of 1-alkynes on Si(100)–H surfaces, see (a) Sieval, A. B.; Opitz, R.; Maas, H. P. A.; Schoeman, M. G.; Meijer, G.; Vergeldt, F. J.; Zuilhof, H.; Sudhölter, E. J. R. *Langmuir* **2000**, *16*, 10359–10368. (b) Cerofolini, G. F.; Galati, C.; Reina, S.; Renna, L. *Surf. Interface Anal.* **2006**, *38*, 126–138. (c) Cerofolini, G. F.; Galati, C.; Reina, S.; Renna, L. *Appl. Phys. A* **2005**, *80*, 161–166. (d) Cerofolini, G. F.; Galati, C.; Reina, S.; Renna, L.; Giannazzo, F.; Raineri, V. *Surf. Interface Anal.* **2004**, *36*, 71–76.

(68) Compound **3** has previously been reported to promote Cu-catalyzed transformations and has been successfully used as a bidentate ligand in the coupling of imidazoles with arylboronic acids. (Collman, J. P.; Zhong, M.; Zhang, C.; Costanzo, S. J. *Org. Chem.* **2001**, *66*, 7892–7897.)

(69) Benesch, J.; Svedhem, S.; Svensson, S. C. T.; Valiokas, R.; Liedberg, B.; Tengvall, P. *J. Biomater. Sci., Polymer Ed.* **2001**, *12*, 581–597.

(70) Sharma, S.; Johnson, R. W.; Desai, T. A. *Langmuir* **2004**, *20*, 348–356.

(71) Zhu, X.-Y.; Jun, Y.; Staarup, D. R.; Major, R. C.; Danielson, S.; Boiadjev, V.; Gladfelter, W. L.; Bunker, B. C.; Guo, A. *Langmuir* **2001**, *17*, 7798–7803.

(72) Prime, K. L.; Whitesides, G. M. *J. Am. Chem. Soc.* **1993**, *115*, 10714–10721.

(73) Lasseter, T. L.; Clare, B. H.; Abbott, N. L.; Hamers, R. J. *J. Am. Chem. Soc.* **2004**, *126*, 10220–10221.

scans and selecting a resolution of 2 cm⁻¹. Azide **2c** was synthesized from tetra(ethylene glycol) via the corresponding monotosylated derivative according to literature procedures with minor modifications.^{74,75}

Preparation of 1-Azidobutane (2a).⁷⁶ To sodium azide (17.2 g, 0.25 mol) in 50 mL of a water/methanol mixture (7:3) was added 1-bromobutane (34.5 g, 0.25 mol), and the reaction mixture was stirred at 60 °C for 24 h. The resulting mixture was washed with brine (2 × 25 mL), and subsequent fractional distillation afforded the intended azide (boiling range 106–108 °C) as a colorless liquid (11.7 g, 0.118 mol, 47%): ¹H NMR (300 MHz, CDCl₃) δ 0.95 (t, *J* = 7.5 Hz, 3H), 1.41 (m, 2H), 1.83 (m, 2H), 3.25 (t, *J* = 6.9 Hz, 2H). ¹³C NMR (300 MHz, CDCl₃) δ 50.1, 32.6, 19.7, 13.5. IR (neat). 1116, 1215, 1262, 1279, 1351, 1380, 1465, 1633, 2097, 2874, 2934, 2962.

Preparation of 2-{2-[2-(2-Azidoethoxy)ethoxy]ethoxy}ethanol (2c).⁷⁶ To a solution of anhydrous pyridine (4 mL) and anhydrous dichloromethane (20 mL) was added tetra(ethylene glycol) (Aldrich, ~99%) (5 g, 29 mmol). The solution was stirred and cooled to -10 °C under an argon atmosphere. A solution of *p*-toluenesulfonyl chloride (1 g, 5 mmol) in dry dichloromethane (10 mL) was added dropwise over 1 h with stirring. The resultant mixture was stirred at room temperature for 20 h (reaction monitored by TLC, dichloromethane/methanol 5:1). The reaction mixture was evaporated under reduced pressure, and the crude material was purified using silica gel column chromatography (dichloromethane/methanol 10:1) to afford 2-{2-[2-(2-hydroxyethoxy)ethoxy]ethoxy}ethyl 4-methylbenzenesulfonate (monotosylated glycol) as a colorless oil (1.243 g, 3.57 mmol, 71%): ¹H NMR (300 MHz, CDCl₃) δ 2.42 (s, 3H), 2.66 (br s, 1H), 3.63 (m, 14H), 4.13 (t, *J* = 5.0 Hz, 2H), 7.32 (d, *J* = 8.2 Hz, 2H), 7.76 (d, *J* = 8.2 Hz, 2H). ¹³C NMR (300 MHz, CDCl₃) δ 144.74, 132.84, 129.73, 127.82, 72.39, 70.55, 70.48, 70.28, 70.14, 69.16, 68.54, 61.50, 21.5. IR (neat) 1176, 1247, 1292, 1355, 1425, 1597, 1724, 2874, 3457.

To a solution of the monotosylated glycol (0.989 g, 2.84 mmol) in *N,N*-dimethylformamide (10 mL) and water (7 mL) was added sodium azide (2.94 g, 45 mmol). The resultant suspension was warmed to 60 °C in an oil bath and stirred overnight. The mixture was evaporated under reduced pressure, and the resulting residue was suspended in 80 mL of ethyl acetate. The suspension produced was filtered, and the filtrate was concentrated. The crude product was purified using silica-gel chromatography (ether) to give substituted azide **2c** as a colorless oil (0.373 g, 1.7 mmol, 60%): ¹H NMR (300 MHz, CDCl₃) δ 3.07 (br s, 1H), 3.36 (t, *J* = 4.9 Hz, 2H), 3.57 (t, *J* = 4.9 Hz, 2H), 3.66 (m, 12H). ¹³C NMR (300 MHz, CDCl₃) δ 72.41, 70.53, 70.51, 70.42, 70.18, 69.87, 61.54, 50.55. IR (neat) 1120, 1286, 2096, 2870, 3437.

Assembly of Monolayers of 1,8-Nonadiyne (1). Silicon wafers were cut into pieces (approximately 10 × 18 mm²) and cleaned for 30 min in hot Piranha solution (100 °C, 1 vol 30% by mass aqueous hydrogen peroxide to 3 vol sulfuric acid), before being transferred to an aqueous fluoride solution (2.5% hydrofluoric acid, 1.5 min). Subsequently, the samples were transferred, taking extra care to exclude air completely from the reaction vessel (a custom-made Schlenk flask), to a degassed (through a minimum of 4 freeze-pump-thaw cycles) sample of diyne **1**. The sample was kept under a stream of argon while the reaction vessel was immersed in a oil bath set to 170 °C for 3 h. The flask was then opened to the atmosphere, and the functionalized surface sample (surface 1, Scheme 1) was rinsed consecutively with copious amounts chloroform, ethyl acetate, and then ethanol before being either analyzed or further reacted with substituted azide species.

Click Derivatization of the Acetylene-Terminated Si(100) Surface. In a typical click procedure, to a reaction vial containing the alkyne-functionalized silicon surface (samples had an average

Table 1. Click Reactions on Acetylene-Terminated Si(100) Surfaces

entry	alkyne	azide	triazole product	ligand 3	<i>T</i> /°C	<i>t</i> /h	yield ^a
1	surface 1	2a	surface 2		25	18	80
2	surface 1	2b	surface 3		r.t.	17	76 ^b
3	surface 1	2c	surface 4	1 mol %	r.t.	10	48
4	surface 1	2c	surface 4		r.t.	10	36
5	surface 1	2c	surface 4	1 mol %	r.t.	18	51
6	surface 1	2c	surface 4		r.t.	18	42
7	surface 1	2c	surface 4	1 mol %	r.t.	40	54
8	surface 1	2c	surface 4		r.t.	40	50

^a Approximate yields, based on XPS-derived elemental analysis values, are reported in % on the basis of alkyne conversion to the triazole product. ^b Yields calculated for the HCl-treated surface sample.

surface area of 120 mm²) were added (i) the azide (**2a–2c**, 10 mM, ethanol/water 1:1), (ii) copper(II) sulfate pentahydrate (1 mol % relative to the azide), and (iii) sodium ascorbate (25 mol % relative to the azide). Reactions were carried out at room temperature,⁷⁷ without excluding air from the reaction environment, and stopped after 17 to 18 h. The prepared surface-bound [1,2,3]-triazole samples were rinsed consecutively with copious amounts of ethyl acetate, ethanol, and water and then analyzed. The variation in the reaction times was investigated for surface 4 only (entries 3–8, Table 1). The only deviation from the standard click procedure was in the addition to the reaction mixture of 1 mol % (relatively to the azide) *N,N,N',N'*-tetramethylethane-1,2-diamine (**3**). The effect of the presence of amine **3** on the cycloaddition reaction was evaluated only for the preparation of surface 4 (entries 3, 5, and 7; Table 1).

XPS Measurements. X-ray photoelectron spectroscopy data were acquired using an ESCALAB 220iXL spectrometer with a monochromatic Al K α source (1486.6 eV), hemispherical analyzer, and multichannel detector. Spectra were recorded in normal emission with the analyzing chamber operating below 10⁻¹⁰ mbar and selecting a spot size of approximately 1 mm². The angle of incidence was set to 58° with respect to the analyzer lens. The resolution of the spectrometer is ~0.6 eV as measured from the Ag 3d_{5/2} signal (full width at half maximum, fwhm). All energies are reported as binding energies in electron volts and referenced to the Si 2p_{1/2} signal (corrected to 99.9 eV). Survey scans were carried out over the 1100–0 eV range with a 1.0 eV step size, a 100 ms dwell time, and an analyzer pass energy of 100 eV. The Br 3d (63–75 eV), Si 2p (97–107 eV), C 1s (278–294 eV), N 1s (392–408 eV), O 1s (526–542 eV), and Cu 2p_{3/2} (926–938 eV) regions were investigated in detail. High-resolution scans were run with a 0.1 eV step size, a dwell time of 100 ms, and the analyzer pass energy set to 20 eV. The Cu LMM region (Auger transition, 562–582 eV) was investigated for surface 4 only.

Analysis of the spectra involved background subtraction using the Shirley routine and a subsequent nonlinear least-squares fitting to mixed Gaussian–Lorentzian functions.⁷⁸ Data from the C 1s emission region were fitted to functions having 80% Gaussian and 20% Lorentzian character. A different weighting of these functions was used, depending on the chemical composition of the organic layer. The N 1s spectral region was deconvoluted and fitted to two peaks held 1.4 eV apart, each composed of a 100% Gaussian line shape. Signals ascribed to the Si 2p emission were fitted to two 95% Gaussian/5% Lorentzian functions held ~0.6 eV apart.⁷⁹ Decomposition of the Cu 2p_{3/2} signal to assign Cu(II) and Cu(I) contributions was based on literature procedures.⁸⁰ The calculated Auger parameter for the residual copper catalyst (following the determination of both

(77) Coupling reaction of surface 1 with 1-azidobutane **2a** to afford surface 2 was performed with the reaction vessel immersed in a water bath set to 25 °C.

(78) XPS spectra were analysed using freeware software XPSpeak developed by Dr. Raymond Kwok, Department of Chemistry, The Chinese University of Hong Kong.

(79) Bansal, A.; Li, X.; Yi, S. I.; Weinberg, W. H.; Lewis, N. S. *J. Phys. Chem. B* **2001**, *105*, 10266–10277.

(80) (a) Meda, L.; Cerofolini, G. F. *Surf. Interface Anal.* **2004**, *36*, 756–759. (b) Meda, L.; Raghino, G.; Moretti, G.; Cerofolini, G. F. *Surf. Interface Anal.* **2002**, *33*, 516–521.

(74) Xie, H.; Braha, O.; Gu, L.-Q.; Cheley, S.; Bayley, H. *Chem. Biol.* **2005**, *12*, 109–120.

(75) Shirude, P. S.; Kumar, V. A.; Ganesh, K. N. *Eur. J. Org. Chem.* **2005**, 5207–5215.

(76) Synthesis schemes for the preparation of compounds **2a** and **2c** are included in Supporting Information.

Auger and photoelectron lines for the metal) was compared to tabulated values reported in Wagner's plots for Cu(I) species.⁸¹ Atomic compositions of the prepared surface samples were corrected for the number of scans accumulated and for the atomic sensitivity of the element. Atomic sensitivities were 2.841 for Br(3d), 0.328 for Si(2p), 0.278 for C(1s), 0.477 for N(1s), 0.78 for O(1s), and 9.78 for Cu(2p). XPS data for surfaces 2 and 4 (entries 1, 3, and 4; Table 1) were acquired at the Brisbane Surface Analysis Facility, The University of Queensland, using a Kratos Axis Ultra X-ray photoelectron spectrometer incorporating a 165 mm hemispherical electron-energy analyzer. The incident radiation was monochromatic Al K α X-rays (1486.6 eV) at 45° to the sample surface. Photoelectron data were collected at a takeoff angle of 90°. For survey and high-resolutions scans, the analyzer pass energy was set to 160 and 20 eV, respectively. Survey scans were carried out over the 1200–0 eV binding-energy range with 1.0 eV steps and a dwell time of 100 ms. Narrow, high-resolution scans were run with 0.05 eV steps and a 250 ms dwell time. The base pressure in the analysis chamber was 1.0×10^{-9} Torr, and during sample analysis, it was 1.0×10^{-8} Torr.

The ratios of the integrated areas for the C 1s and N 1s emissions, each normalized for their elemental sensitivity and scanning time (number of scans accumulated), afforded an estimate of the conversion of the acetylene-terminated surface to the intended triazole product.⁸²

XRR Measurements. X-ray reflectivity profiles were measured for functionalized surfaces 1, 3, and 4 on a Panalytical Ltd X'Pert Pro reflectometer using Cu K α X-ray radiation ($\lambda = 1.54056 \text{ \AA}$) produced from a 45 kV tube source. The X-ray beam was focused using a Göbel mirror and collimated with 0.2 mm pre- and postsample slits and a De-Wolf beam knife mounted above the sample to reduce the sample footprint at very low angles. The reflected X-rays were counted using a NaI scintillation detector. Reflectivity data were collected over the angular range of $0.05^\circ \leq \theta \leq 4.00^\circ$, with a step size of 0.010° and a counting time of 15 s per step. (θ is the angle of incidence of the X-ray beam impinging upon the surface.) Samples had an average size of $10 \times 30 \text{ mm}^2$. Structural parameters of the prepared organic thin layers were refined using MOTOFIT reflectivity analysis software⁸³ with reflectivity data as a function of the momentum transfer vector Q_z ($Q_z = 4\pi(\sin\theta)/\lambda$). In the fitting routines, the scattering length density of the silicon substrate was held at $2.01 \times 10^{-5} \text{ \AA}^{-2}$, and the Levenberg–Marquardt method was selected to minimize χ^2 values.⁸⁴ Single-layer models were proposed when no significant improvement in the fitting quality was observed upon the introduction of an additional layer into the refined model.

Water Contact Angle Measurements. Water contact angles were determined on a Ramé-Hart 100-00 goniometer. All samples were prepared in triplicate with at least three separate spots being measured for each sample. The reproducibility of the contact angle measurements was $\pm 2\text{--}4^\circ$.

Protein Adsorption Assays. Nonspecific adsorption of fluorescein isothiocyanate-labeled bovine serum albumin (FITC-BSA) on the functionalized surface samples, relative to the hydrogen-terminated silicon surface, was evaluated for surfaces 1 and 4, according to the procedure described by Clare et al.⁸⁵ Briefly, samples (with an average surface area of 120 mm^2) were exposed for a 1 h period to a labeled protein solution (0.1% FITC-BSA, 0.1 M NaHCO₃, pH 8.3). The samples were subsequently rinsed with copious amounts of Milli-Q water and then incubated with the elution buffer (0.3 M NaCl, 20 mM Na₂HPO₄, 2 mM EDTA, 1% Triton X-100, 1% β -mercapto-

ethanol, pH 7.4.) for 16 h. Fluorescence intensities ascribed to the labeled protein eluted from the surface were measured on a Perkin-Elmer LS 50B spectrofluorometer using a $490 \pm 10 \text{ nm}$ excitation source and recording the fluorescence at $520 \pm 10 \text{ nm}$. Samples were prepared in triplicate, and for each sample, a minimum of three repeated fluorescence measurements were obtained. The 95% confidence limit of the mean was calculated to be $t_{n-1}s/n^{1/2}$ where $t_{n-1} = 4.3$, s is the standard deviation, and n is the number of repeated measurements.⁸⁶ Fluorescence intensities were normalized to those observed for the hydrogen-terminated Si(100) surface samples and corrected for the sample surface.

Results

Assembly of Monolayers of 1,8-Nonadiyne 1 on Hydrogen-Terminated Si(100) Surfaces (Surface 1). The thermally induced hydrosilylation reaction of anhydrous diacetylene species **1** on freshly etched Si(100) surfaces produced surface 1 as determined using XPS, XRR, and contact angle measurements. An advancing water contact angle, Θ_a , for acetylene-terminated surface 1 of $87 \pm 3^\circ$, was consistent with the presence of a hydrophobic monolayer but was considerably smaller (by $\sim 20\text{--}30^\circ$) than those reported for analogous methyl-terminated monolayers prepared on Si(100) from 1-alkenes and 1-alkynes.⁹ This observation was consistent with the higher polarizability of the acetylene moieties relative to that of methyl groups, which results in a more hydrophilic surface.

XPS spectra acquired on the acetylene-terminated surface are shown in Figure 1. The survey spectrum indicated the presence of Si, C, and O, which is in good agreement with the presence of an organic monolayer on the silicon substrate (Figure 1a).^{67b–d,87} The oxygen 1s emission at $\sim 532 \text{ eV}$ is ascribed to adventitiously adsorbed oxygen. The narrow scan of the C 1s region (Figure 1b) showed a broad signal with a mean binding energy of 285.0 eV. The large dispersion value (1.54 eV fwhm) of the fitted function (Figure S1, Supporting Information) was consistent with a peak resulting from contributions of carbon-, hydrogen-, and silicon-bonded carbon atoms being either sp-, sp²- or sp³-hybridized. Given the chemical composition of the monolayer assembled from diyne **1**, no further deconvolution of the C 1s signal was proposed. Contributions from carbon atoms in the C–Si bonding configurations could not be assigned unambiguously because the quality of the fit was not improved by adding a satellite peak centered at $\sim 284.1 \text{ eV}$ representing slightly negatively charged carbon atoms (Si–C–R₁R₂R₃; R₁, R₂, R₃ = C, H).⁸⁸ Nevertheless, an observed inflection point at $\sim 283.9 \text{ eV}$ suggests the presence of a lower-energy shifted contribution from silicon-bonded carbons, consistent with previous reports.⁸⁹ In the Si 2p narrow scan (Figure 1c; Figure S1, Supporting Information) of surface 1, no significant oxide or suboxide silicon was detected in the 101–104 eV region.^{90,91} The absence of any significant level of oxide is indicative of a well-formed monolayer effectively preventing the ingress of air to the silicon substrate.^{65c}

(86) Miller, N. J.; Miller, C. J. *Statistics and Chemometrics for Analytical Chemistry*; Prentice Hall: Harlow, England, 2000.

(87) (a) Sun, Q.-Y.; de Smet, L. C. P. M.; van Lagen, B.; Giesbers, M.; Thüne, P. C.; van Engelenburg, J.; de Wolf, F. A.; Zuilhof, H.; Sudhölter, E. J. R. *J. Am. Chem. Soc.* **2005**, *127*, 2514–2523. (b) de Smet, L. C. P. M.; Pukin, A. V.; Sun, Q.-Y.; Eves, B. J.; Lopinski, G. P.; Visser, G. M.; Zuilhof, H.; Sudholter, E. J. R. *Appl. Surf. Sci.* **2005**, *252*, 24–30.

(88) (a) Nemanick, E. J.; Hurley, P. T.; Webb, L. J.; Knapp, D. W.; Michalak, D. J.; Brunschwig, B. S.; Lewis, N. S. *J. Phys. Chem. B* **2006**, *110*, 14770–14778. (b) Wallart, X.; de Villeneuve, C. H.; Allongue, P. *J. Am. Chem. Soc.* **2005**, *127*, 7871–7878. (c) Liu, H.; Hamers, R. *J. Surf. Sci.* **1998**, *416*, 354–362.

(89) Ishizaki, T.; Saito, N.; SunHyung, L.; Ishida, K.; Osamu, T. *Langmuir* **2006**, *22*, 9962–9966.

(90) Himpfel, F. J.; McFeely, F. R.; Taleb-Ibrahimi, A.; Yarmoff, J. A. *Phys. Rev. B* **1988**, *38*, 6084–6096.

(91) Lehner, A.; Steinhoff, G.; Brandt, M. S.; Eickhoff, M.; Stutzmann, M. *J. Appl. Phys.* **2003**, *94*, 2289–2294.

(81) Wagner, C. D.; Joshi, A. J. *Electron Spectrosc. Relat. Phenom.* **1988**, *47*, 283–313.

(82) A parallel approach to evaluate reaction yields relied on a comparison between XPS C 1s intensities (integrated area of the corresponding fitted function) ascribed to atoms in different environments. Given that good agreement was generally observed between the two approaches used to quantitate the immobilization of azide species, for clarity, results from only the N/C elemental analysis method are reported in the text.

(83) Nelson, A. J. *Appl. Crystallogr.* **2006**, *39*, 273–276.

(84) Flannery, B. P.; Teukolsky, S. A.; Vetterling, W. T. *Numerical Recipes in C*; Cambridge University Press: Cambridge, England, 1988.

(85) Lasseter, T. L.; Clare, B. H.; Nichols, B. M.; Abboth, N. L.; Hamers, R. *J. Langmuir* **2005**, *21*, 6344–6355.

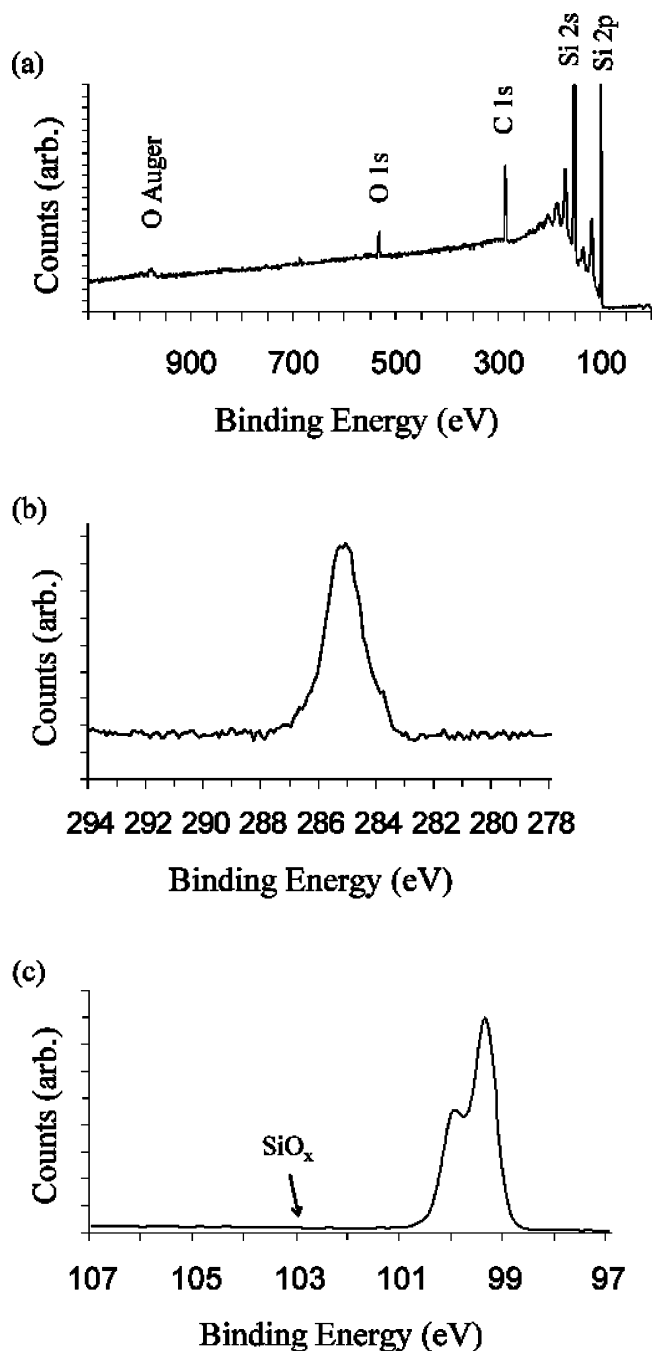


Figure 1. XPS spectra of monolayers assembled from diyne **1** on a hydrogen-terminated Si(100) (surface 1). (a) Survey spectrum. (b) Narrow scan of the C 1s region. (c) High-resolution scan for the Si 2p region. Absent from the spectra is the signal associated with SiO_x.

To gain structural information on the monolayers prepared from diyne **1**, XRR spectra were recorded. The observed (points) and calculated (solid line) X-ray reflectivity profiles are shown in Figure 2a, where the calculated reflectivity profile is generated from the refined structural model (Table 2). As expected for very thin films (~ 1 nm), only one minimum in the Kessig fringes (resulting from interference between X-rays reflecting off of the air–film and film–silicon interfaces) was observed before the signal merged into the background. The refined thickness (d) of the monolayer was found to be 12(1) Å. Comparison with the calculated length of 12.22 Å⁹² for the acetylene-terminated

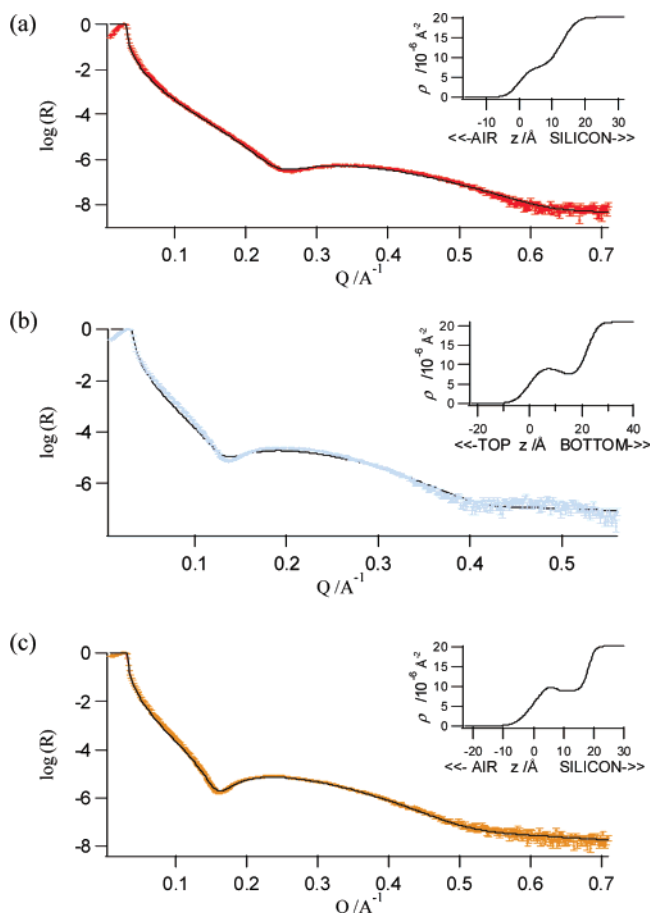


Figure 2. X-ray reflectometry spectra acquired on organic modified Si(100) surfaces. (a) Acetylene-terminated monolayers (surface 1), (c) Azidophenacyl bromide-derived sample (surface 3). (b) Tetra(ethylene oxide)-functionalized organic layer (surface 4; entry 6, Table 1). The refinement of a structural model (solid line) is always proposed. The inset in each plot shows a depth-profile view of the refined SLDs (scattering-length densities).

Table 2. Refined Structural Parameters from XRR Data^a

	surface 1	surface 3		surface 4	
		layer 1	layer 2	layer 1	layer 2
σ_{silicon} (Å)	3(1)	3(1)		4(1)	
$\sigma_{\text{monolayer}}$ (Å)	3(1)	3(1)	3(1)	2(1)	3(1)
d (Å)	12(1)	11(1)	11(1)	11(1)	7(1)
ρ_{el} (e ⁻ Å ⁻³)	0.27(2)	0.25(2)	0.35(2)	0.26(2)	0.38(2)

^a Estimated standard deviations (esd's) are given in parentheses.

monolayer indicates that the chain axis of molecules in the monolayer is essentially normal to the surface. Furthermore, the consistency between the measured and calculated lengths of the molecules indicates that there is no hairpinning of the dialkyne such that both ends are attached to the silicon surface. The electron density (ρ_{el}) of the organic layer was also derived from the XRR data (Table 2). The refined electron density obtained for the acetylenyl surface (~ 0.27 e⁻/Å³)⁹³ was lower than the average 0.31 e⁻/Å³ reported for a series of methyl-terminated monolayers prepared on Si(100) from 1-alkynes.^{67a} On the basis of both the obtained monolayer thickness and the value of the electron density, XRR data enabled the calculation of the molecular coverage of the silicon surface as 21(2) Å² per grafted molecule. Both values of the refined interfacial roughness (σ_{silicon} and $\sigma_{\text{monolayer}}$) were

(93) SLD for X-rays is obtained by multiplying the electron density (e⁻/Å³) of the material by the factor 2.82×10^{-5} Å.

(92) Semi-empirical MOPAC calculation (Chem3D Ultra).

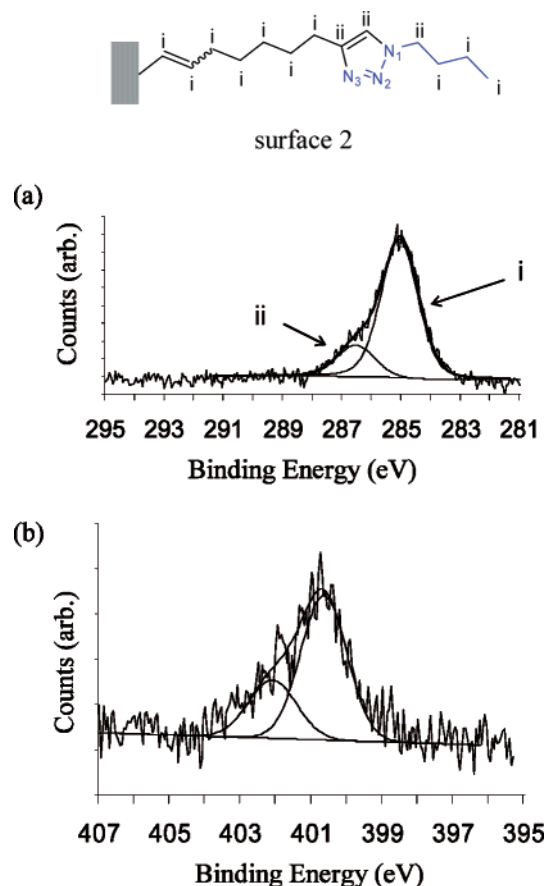


Figure 3. High-resolution XPS spectra of the surface-bound [1,2,3]-triazole species (surface 2, entry 1, Table 1) prepared using the click reaction of azido compound **2a** with acetylene-terminated silicon surfaces. (a) C 1s high-resolution data showing a high-energy contribution (~ 286.5 eV) ascribed to carbon atoms directly bonded to nitrogen atoms in the [1,2,3]-triazole moiety, schematically depicted as ii. (b) Narrow scans for the N 1s region indicative of the formation of the triazole moiety.

found to be $3(1)$ Å, which reflects a very high quality monolayer film on atomically flat polished silicon.^{5,15,65b}

The combined XPS and XRR data were consistent with a well-formed, densely packed monolayer effectively passivating the underlying silicon substrate as the result of a facile, noncatalyzed, thermal hydrosilylation of a diacetylene species with hydrogen-terminated Si(100) as the reactive substrate.

Click Functionalization of Alkyne-Terminated Monolayers.

The utility and generality of the click approach to introduce chemical functionalities specifically onto organic-passivated silicon surfaces were illustrated by reacting the alkyne-terminated silicon surface with three representative azide species (**2a–2c**).

Butyl-Terminated Surfaces (Surface 2). The coupling of 1-azidobutane (**2a**) onto the alkyne-terminated silicon surfaces, thus affording surface 2 (entry 1, Table 1), was primarily for XPS to aid in assigning peaks and establishing the fitting routine used. The lack of carbon–oxygen bonds in this surface-bound triazole derivative allowed a simplified and unambiguous assignment of the contributions to the observed C 1s emission from nitrogen-bonded (C–N)⁹⁴ and carbon-bonded (C–C) carbon atoms (Figure 3). Given the chemical composition of organic layers prepared using click immobilization of azide **2a** onto acetylenyl silicon surfaces, no other carbon populations are

(94) The observed XPS spectral position for nitrogen-bonded carbons was found to be in good agreement with binding-energy values reported by Böcking et al. for analogous carbon atoms (~ 286.4 eV).⁵

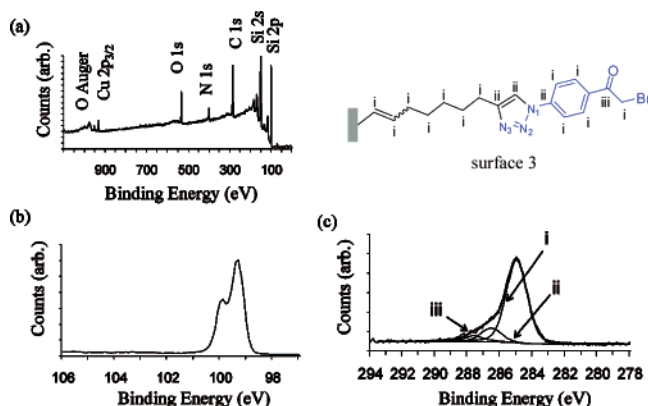


Figure 4. XPS analysis of surface 3 (entry 2, Table 1). (a) XPS survey spectrum. (b) Narrow scan of the Si 2p region showing no detectable levels of SiO_x species (102–104 eV), thus indicating negligible oxidation of the underlying silicon substrate during the cycloaddition process. (c) XPS narrow scans of the C 1s region after background subtraction and peak fitting to assign contributions to the spectrum from carbon atoms in different environments (C–C, C–N, and C=O designated as i, ii, and iii, respectively).

expected to be present on the functionalized surface and thus contribute to the C 1s XPS signal.

Deconvolution of the recorded C 1s narrow scan into its putative contributions (Figure 3a) suggested a 1.5 eV peak center-to-center distance between the C–N (~ 286.5 eV, ii in Figure 3) and C–C (~ 285 eV, i in Figure 3) signals with a large dispersion value (1.5 eV fwhm) for the fitted C–N function. Photoelectrons emitted from carbon atoms present in any unreacted alkyne and from the equivalent atoms in the surface-bound [1,2,3]-triazole product contributed to peak i only.

The high-resolution N 1s data (Figure 3b) showed a broad peak centered at ~ 401 eV, suggesting the presence of chemically distinct nitrogen atoms consistent with the formation of a triazole moiety and strongly supporting the fusion of azide species **2a** to the acetylene-decorated surface.^{45,53} The best fit to the experimental N 1s emission curve was obtained when this spectral region was deconvoluted into two functions having binding energies of 402.2 and 400.7 eV and with a 1:2 ratio of the integrated areas. If any unreacted azide species was physically absorbed in the monolayer, then a well-resolved peak at ~ 405 eV corresponding to the electron-deficient nitrogen in the azide group would be expected.⁴⁶ No such peak was observed in our spectrographs.

On the basis of nitrogen and carbon XPS-derived elemental analysis values, a conversion of approximately 80% of the acetylene-terminated surface to the triazole product was calculated.

Phenacylbromide-Terminated Surfaces (Surface 3). Evidence of a successful click reaction of aryl azide **2b** with surface acetylenes (entry 2, Table 1) was provided by contact angle measurements showing a 10° decrease in the advancing contact angle value ($\Theta_a = 77 \pm 3^\circ$) relative to analogous data obtained for surface 1. The increased hydrophilicity was consistent with the acyl bromide moiety being present on the derivatized surface.

That the change in contact angle was due to the formation of a [1,2,3]-triazole ring was confirmed using XPS. XPS survey scans (Figure 4a) showed the presence of nitrogen and copper species not present on the acetylene-terminated surface. The copper peaks due to Cu 2p_{3/2} photoemission (Figure S2a, upper spectra) at ~ 933 eV can be attributed to the Cu(I) catalyst used in the reaction that was not completely removed using the normal rinsing procedure. These traces of residual copper catalyst were removed upon overnight exposure of surface 2 to a 0.3 M HCl

solution (Figure S2a, lower spectra).⁹⁵ Not easily distinguishable in the wide scan but visible in high-resolution scans was a peak of mean binding energy of ~ 71.3 eV ascribed to the Br 3d emission and consistent with a positive outcome of the immobilization of azide **2b** onto surface 1 (Figure S2b). The lack of detectable high-energy (102–104 eV) emissions in the Si 2p narrow scans further illustrates the ability of **1** to passivate the silicon surface (Figure 4b).

Important regions of the XPs spectra to confirm that azide **2b** was successfully clicked onto surface 1 were provided by both the C 1s (Figure 4c) and N 1s (Figure S2c) XPS regions. The C 1s peak was deconvoluted into three different contributions using XPS data acquired from surface 2 as a reference for the nitrogen-bonded carbon assignments. The main C 1s signal, centered at ~ 285.1 eV (1.5 eV fwhm) and labeled i in Figure 4c, was attributed to carbon atoms attached to another carbon atom (C–C). Emissions from nitrogen-bonded carbons (C–N) at ~ 286.6 eV ($\Delta E = 1.5$ eV, peak center-to-center distance between the C–N and C–C signals) with a fwhm of 1.5 eV appear as peak ii in Figure 4c. A high-energy contribution at ~ 287.7 eV, associated with the electron-deficient carbon atom in the carbonyl group, C=O (iii in Figure 4c, $\Delta E = 2.6$ eV, 1.4 eV fwhm) was required to achieve satisfactory fits and is consistent with the formation of the intended triazole product.

The XPS N 1s narrow scan (Figure S2c) showed a broad emission centered at ~ 401.1 eV suggesting a contribution to the signal from chemically different nitrogen atoms as expected for atoms in the surface-bound heterocycle. Deconvolution of the nitrogen emission as described for surface 2 gave a satisfactory fit to the experimental data. On some surfaces, physically adsorbed azide was identified through the presence of a weak satellite peak at ~ 404.7 eV (Figure S2d).

XPS elemental analysis performed on HCl-treated samples to ensure that any contaminants were removed indicated that $\sim 76\%$ of the surface alkynes were successfully clicked to aryl azide species **2b**.

X-ray reflectivity measurements performed on surface 3 were fitted to a bilayer structural model (Figure 2b), with the refined structural model summarized in Table 2. The thickness of the inner layer was $11(1)$ Å, which is in good agreement with the refined values obtained from surface 1. The thickness of the outer layer was also found to be $11(1)$ Å. The refined total thickness of the organic layer (~ 22 Å) is consistent with a significant conversion of the acetylene-terminated surface to the corresponding triazole product, presenting a phenacylbromide moiety that has a theoretical thickness of 22.2 Å.⁹² XRR data suggest an area per molecule for grafted aryl azide **2b** of $30(3)$ Å², indicating a process yield close to 70%, which correlates well with the X-ray photoelectron spectroscopy data.

Tetra(ethylene oxide)-Terminated Monolayer (Surface 4).

The reaction of surface 1 with azide **2c** (entry 6, Table 1) resulted in a dramatic decrease in the advancing contact angle value from $87 \pm 3^\circ$ for surface 1 to $54 \pm 4^\circ$ for surface 2. Rendering the surface hydrophilic is consistent with the coupling of the oligo

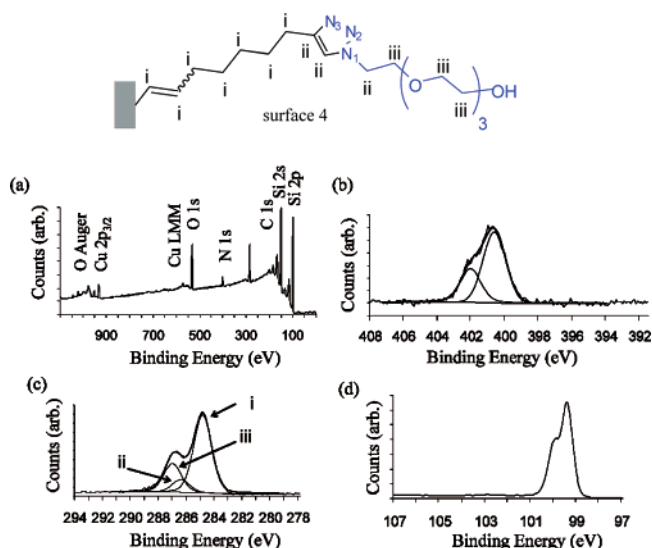


Figure 5. XPS spectra of monolayers of diyne **1** reacted with compound **2c** to form the corresponding surface-bound [1,2,3]-triazole derivative (surface 4, entry 6, Table 1). (a) XPS survey spectrum. (b) XPS narrow scan of the N 1s region. (c) XPS narrow scan of the C 1s region after background subtraction and deconvolution of the spectrum into its putative contributions; namely, C–C, C–N, C–O, indicated as i, ii, and iii and found at ~ 285 , ~ 286.5 , and ~ 287 eV, respectively. (d) Si 2p narrow scan showing negligible levels of SiO_x species formed upon the click step.

ether moieties to the surface and is in good agreement with values observed for similar surfaces prepared on Si(111).^{15,96}

The XPS survey spectrum of surface 4 (Figure 5a) showing the presence of a broad N 1s peak at ~ 401 eV was indicative of successful triazole formation (Figure 5b). Emissions from the C 1s core levels were deconvoluted and fitted to three functions: (i) the main C–C peak centered at ~ 285 eV (1.5 eV fwhm) and referred to as i in Figure 5c, (ii) a nitrogen-bonded carbon (C–N) peak at ~ 286.5 eV (1.5 eV fwhm), with the signal depicted as ii in Figure 5c, and (iii) oxygen-bonded carbon (C–O) emission at 287.1 eV (1.4 eV fwhm), labeled as peak iii in Figure 5c. Furthermore, Si 2p narrow scans acquired from the functionalized surface showed no evidence of oxidation of the substrate during the click step (Figure 5d). XPS data obtained for surface 4 suggested approximately 42% conversion of surface acetylenes after 18 h when substituted oligoether species **2c** was used in the click procedure (entry 6, Table 1).

A significant Cu 2p_{3/2} emission at ~ 933 eV ($\sim 0.1\%$ of the total carbon) was also generally observed in survey scans and was associated with traces of residual copper catalyst despite copious rinsing (Figure 6a, upper spectra). Complete removal of copper traces required overnight exposure of the triazole-functionalized sample to a 0.05% (w/v) ethylenediaminetetraacetic acid solution (pH 8) (Figure 6b, lower spectra).⁹⁷ The relative abundance of Cu(I) and Cu(II) species was assessed on the basis of the decomposition procedure of the Cu 2p_{3/2} photoelectron emission (to which both species contribute) as proposed by Meda et al.⁸⁰ As shown in Figure 6a, a high-quality fit (reduced χ^2) to the experimental curve required a two-function model (100% Gaussian lines). The integrated area (after Shirley background subtraction) under the relatively narrow (1.7 eV

(95) Despite the hydrolytic stability of the triazole moiety being well documented,²⁹ concerns existed regarding the possibility of an ipso ("at the same") substitution reaction at the surficial silylated olefin, the putative interfacial species, [(a) Cerofolini, G. F.; Galati, C.; Reina, S.; Renna, L. *Semicond. Sci. Technol.* **2003**, *18*, 423–429], eventually leading to the complete removal of the entire organic assembly. As a result of the ability of silicon atom to stabilize a positive charge in the beta position, the carbocation originated upon protonation of the double bond affords a weakened carbon–silicon bond that is rapidly cleaved by nucleophiles [(b) Clayden, J.; Greeves, N.; Warren, S.; Wothers, P. *Organic Chemistry*; Oxford University Press: New York, 2001; Chapter 47]. We thus evaluated the effect on exposure of surface 3 to 0.3 HCl, but no evidence of an ipso product (degraded monolayer) was found.

(96) Yam, C. M.; Lopez-Romero, J. M.; Gu, J.; Cai, C. *Chem. Commun.* **2004**, 2510–2511.

(97) Exposure of the triazole-functionalized surface to an aqueous, alkaline (pH 8) EDTA solution did not result in the evident appearance of SiO_x species as indicated by XPS Si 2p narrow scans. (Figure S3). This strongly supports the presence of a densely packed acetylene-terminated monolayer effectively passivating the silicon surface.

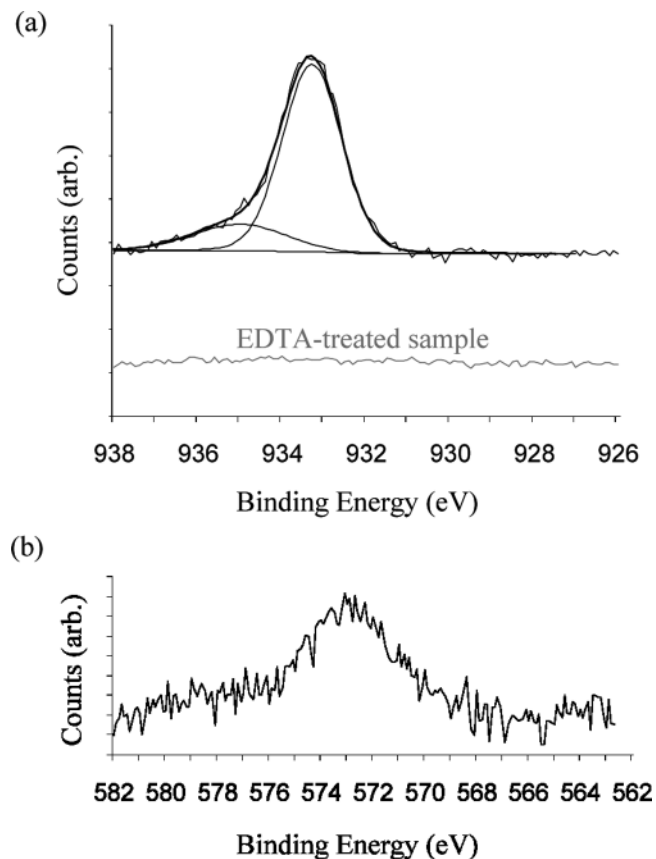


Figure 6. XPS narrow scans of the Cu $2p_{3/2}$ and LMM (Auger) regions for tetra(ethylene glycol)-functionalized surfaces (surface 4, entry 6, Table 1). (a) Deconvolution of the experimental curve for Cu $2p_{3/2}$ emission supports the presence of a predominant Cu(I) population. Traces of residual copper catalyst (upper spectrum) were effectively removed through exposure of the modified surface to a 0.05% EDTA solution (lower spectrum). Spectra are shown offset for clarity. (b) Auger signal of the Cu LMM line with an evident peak at ~ 572.8 eV.

fwhm) signal centered at 933.3 eV, ascribed to Cu(I) species, was compared to the integrated area under the broader Cu(II) contribution (2.54 eV fwhm) at 935 eV to give an 8:1 ratio for the Cu(I)/Cu(II) couple. The Auger copper parameter derived from the relative spectral positions of the Cu LMM Auger line (~ 572.8 eV, Figure 3b) and the Cu $2p_{3/2}$ photoelectron signal (~ 933 eV) was consistent with a predominant Cu(I) population. The calculated Auger parameter, close to 1847.5, was plotted in a Wagner diagram to compare our experimental data with those reported for various Cu(I) salts.⁸¹ The obtained XPS data strongly suggested the ability of the organic modified surface to chelate Cu(I) ions. This complexation of the Cu(I) catalyst may be the cause of the lower coupling yield relative to that of surfaces 2 and 3.

The X-ray reflectivity data for surface 4 is shown in Figure 2c. The solid line is calculated from a two-layer model required give the best fit to the experimental XRR data. The obtained refined structural parameters are listed in Table 2. Upon addition of compound **2c** to surface 1, a second layer of 7(1) Å thickness was attached to the 11(1)-Å-thick underlying layer. The thickness of the prepared organic layer (surface 4) was therefore found to be ~ 18 Å. This thickness is significantly smaller than the calculated length for the expected [1,2,3]-triazole product (25 Å),⁹² suggesting a possible collapse of the introduced oligo(ethylene oxide) moiety. The collapse of oligoethylene oxide surfaces is consistent with previous observations on analogously functionalized Si(111).¹⁵ Furthermore, the refined electron density

value, ρ_{el} , for the upper organic layer ($0.38 \text{ e}^{-}\text{Å}^{-3}$) was found to be similar to that in a previous report for low-density poly(ethylene oxide) monolayers prepared on silicon dioxide surfaces⁹⁸ and suggested a surface area occupied by each clicked tetra(ethylene oxide) molecule of $\sim 45 \text{ Å}^2$. This calculated surface density is consistent with the $\sim 50 \text{ Å}^2$ calculated value based on the 42% conversion of the acetylene monolayer to the [1,2,3]-triazole product determined from XPS measurements.

Fluorescence studies to determine the ability of the tetra(ethylene oxide)-terminated silicon surface (entry 6, Table 1) to resist FITC-BSA nonspecific adsorption are reported in Figure S4. The acquired fluorescence data were compared to those obtained for both the hydrogen-terminated surfaces and acetylene-functionalized substrates (surface 1). The presence of the antifouling organic layer imparted a resistance toward protein adsorption. There was a reduction of approximately 75% in the amount of fluorescence-labeled BSA being detected relative to the same quantity measured for the freshly etched Si(100)-H. This level of suppression of protein adsorption was consistent with previous reports on oligo(ethylene oxide)-modified silicon surfaces.^{99,100}

In light of the coupling efficiency for the cycloaddition of azide **2c** compared with that for **2a** and **2b**, further attempts were made to improve coupling yields by investigating longer reaction times and by stabilizing the Cu(I) species to limit complexation by the oligo(ethylene oxide) species. The addition of *N,N,N',N'*-tetramethylethane-1,2-diamine (**3**) to the click reaction was employed as a Cu(I)-stabilizing ligand. Sharpless et al.¹⁰¹ have systematically studied the effect of selected nitrogen-based copper ligands on the click formation of [1,2,3]-triazoles under aerobic, aqueous conditions and have reported a significant rate-accelerating effect for a series of bidentate ligands sharing a common ethane-1,2-diamine feature. We thus explored the effect of diamine **3** on coupling reactions leading to surface 4 under otherwise unaltered reaction conditions. Three sets of experiments were performed (entries 3–8, Table 1) at reaction times of 10, 18, and 40 h in both the presence and absence of ligand **3**. Compound **3** clearly accelerated the rate of the Cu(I)-dependent process for coupling reactions interrupted after a 10 h period (Entries 3,4). In the presence of diamine **3**, the extent of conversion of the acetylene-terminated monolayer to the corresponding triazole product was $\sim 48\%$ compared with a significantly lower $\sim 36\%$ surface coverage observed in the absence of ligand **3**. Upon an 18 h cycloaddition reaction, approximately 51% of the monolayer was successfully functionalized with azide **2c** if diamine **3** was present during the coupling step whereas, as discussed above, yields of the cycloaddition reaction were only $\sim 42\%$ in a typical “ligand-free” procedure. When prolonged reaction times (40 h) were employed, no significant benefits in terms of the final yield of the coupling procedure associated with the presence of ligand **3** were evident ($\sim 54\%$, ligand-assisted reaction; $\sim 51\%$, ligand-free reaction). This latter result indicates that $\sim 50\%$ coupling was the maximum coupling yield that may be achieved with the tetra(ethylene oxide) species **2c** when a base monolayer of close-packed alkyne moieties was employed.

Discussion

Click chemistry for surface modification is beginning to generate enormous interest because of the potential for achieving

(98) Papra, A.; Gadegaard, N.; Larsen, N. B. *Langmuir* **2001**, *17*, 1457–1460.

(99) Böcking, T.; Gal, M.; Gaus, K.; Gooding, J. J. *Aust. J. Chem.* **2005**, *58*, 660–663.

(100) Yam, C. M.; Gu, J.; Li, S.; Cai, C. J. *Colloid Interface Sci.* **2005**, *285*, 711–718.

(101) Chan, T. R.; Hilgraf, R.; Sharpless, K. B.; Fokin, V. V. *Org. Lett.* **2004**, *6*, 2853–2855.

quantitative coupling of species to a surface with no side reactions. Apart from an initial study by Rohde et al.⁵³ that showed a coupling yield of only ~7%, click chemistry on silicon surfaces is yet to be explored in any detail. The main purpose of the study of Rohde et al. was to achieve complete passivation of the silicon surface by reacting every silicon atom with an organic molecule, an objective that was met with quantitative acetylenylation of silicon surface atoms. The low coupling yields were primarily the result of steric crowding of the surface alkyne functionalities. Hence, our investigation of click chemistry on silicon surfaces was designed to answer the following questions: (1) Could click reactions on silicon surfaces be achieved without oxidation of the underlying silicon surface? (2) Could this coupling be achieved at high efficiency? (3) Could click chemistry be applied to the coupling of a variety of species, which would provide the surface with appropriate properties for biosensing?

Our initial results presented here indicate that the answer to all these questions is yes. Symmetrical diyne **1** was chosen for the initial modification of the silicon surface because there was no ambiguity as to what monolayer would form, it was expected to form an effectively passivating monolayer on Si(100), and it was commercially available. The absence of XPS emissions in the 102–104 eV region of the spectrum for surface 1 indicates that the monolayer formed did passivate the silicon surface effectively.^{62,65c} The absence of any significant oxidation of the silicon surface after clicking any of species **2a–2c** onto the silicon surface is further evidence of a well-formed monolayer using diyne **1**. The absence of any significant silicon oxide even after 40 h of exposure to azide **2c** is particularly significant because our previous studies of coupling similar ethylene oxide species to monolayer-modified silicon surfaces showed that it was particularly difficult to avoid oxidation of the silicon surface when this class of molecule was appended.¹⁵ The good passivation of the silicon surface is consistent with the XRR results that indicate a high grafting density consistent with a $70 \pm 6\%$ coverage of silicon atom sites¹⁰² and the monolayer normal to the surface.

The coupling of two azides **2a** and **2b** to the alkyne-terminated surface was reasonably high at 80 and 76%, respectively, with the increased thickness of the monolayer after attaching azide **2b**, as determined using XRR, being consistent with the molecular dimensions. The estimated surface density of the surface dipolarophile of $4.3\text{--}5.3$ molecule nm^{-2} (XRR data) suggested that steric factors were not a significant influence on the click modification of acetylenyl Si(100) surfaces. However, the yield of the coupling of tetra(ethylene oxide) **2c**, although much higher than the 7% observed by Rohde et al.,⁵³ was a significantly lower than for the other azides, being 54% in the best case. There were, however, a number of issues that complicate the coupling of azide **2c** to the alkyne surface. These issues relate to the complexation of the Cu(I) catalyst by the oligo(ethylene oxide) moieties and the fact that these molecules collapse on the surface rather than remaining fully extended. We hypothesize that this collapse of the oligoether on surface 4 limits the coupling yield due to steric constraints introduced upon the formation of neighboring triazoles immobilized on the surface rather than the decreased yield being a limitation of the coupling chemistry itself, a hypothesis that we intend to test through forming mixed monolayers where the terminal alkynes are diluted by a component that will not participate in the click reaction. The use of diamine **3** as a ligand to complex Cu(I) appeared to be effective at reducing the complexation of Cu(I) by oligoether **2c**.

(102) A comparatively higher surface coverage with ~55–60% of the silicon atom sites bearing alkyl chains is reported for high-quality covalent alkyl monolayers prepared on Si(111).^{5,65b}

Finally, in the initial development of this surface chemistry the option existed to have the self-assembled monolayer terminated at the distal end with either an alkyne or an azide. In this study, apart from the fact that the dialkyne used is commercially available, we chose to make the alkyne the surface-bound species for the following reasons. First, if the alkyne is in solution then the possibility exists that the alkyne can coordinate with the Cu(I) catalyst (alkynes have a preference for Cu(I) over azide ligands^{34,103}) and hence reduce the observed reaction rates for the coupling process. Second, the alkyne in solution increases the chance of alkyne homocoupling. Our caution in this regard arose from early solid-phase click combinatorial chemistry applications investigated by Meldal and co-workers that resulted in difficulties in the coupling of alkynes to azide-functionalized resins; these difficulties were reasoned to be a direct consequence of acetylenic cross coupling occurring in the solution phase and negatively affecting the observed yields.^{31,104} We expected similar homocoupling reactions to be highly disfavored in the case of surface-bound alkynes reacted with solution-phase substituted azides.

Conclusions

The results presented in this article have demonstrated the utility of Cu(I)-catalyzed Huisgen-type cycloadditions of azides to an alkyne-terminated monolayer in preparing functionalized surfaces. The method is robust and experimentally straightforward, allowing the introduction of a range of chemical functionalities onto a hydrogen-terminated silicon substrate. In all cases, no oxidation of the underlying silicon substrate was observed, even after exposure to alkaline aqueous environments.

The thermal hydrosilylation of diyne **1** produced Si–C grafted, well-formed, effectively passivated acetylene-terminated monolayers on Si(100). Further derivatization of this organic structure using click chemistry proceeded to afford hydrolytically resistant 1,4-disubstituted surface triazole species through a coupling procedure that did not require protection/activation steps and was generally insensitive to steric factors. A range of azides, with different chemical functionalities, were used in this process without the need to vary the reaction conditions and without any apparent disruption of the base monolayer.

The surfaces produced using this procedure have potential application in areas where the ability to functionalize the surface selectively may be combined with the electronic properties of the silicon substrate.

Acknowledgment. We thank Dr. Barry Wood (Brisbane Surface Analysis Centre, University of Queensland) for help with X-ray photoelectron spectroscopy analysis. We are grateful for support provided by the Australian Research Council. S.C. was supported by an International Postgraduate Research Scholarship from the Australian Government and a UNSW School of Chemistry Award.

Supporting Information Available: Additional XPS spectrographs, synthesis schemes for the preparation of **2a** and **2c**, contact angle values for the prepared organic assemblies, and spectroscopic evaluation of FITC-BSA nonspecifically adsorbed on acetylene- and tetra(ethylene oxide)-functionalized Si(100) surfaces. This material is available free of charge via the Internet at <http://pubs.acs.org>.

LA701035G

(103) Rodionov, V. O.; Fokin, V. V.; Finn, M. G. *Angew. Chem., Int. Ed.* **2005**, *44*, 2210–2215.

(104) For examples of the preparation of 1,3-diyne through homocoupling reactions of terminal alkynes, see (a) Cameron, M. D.; Bennett, G. E. *J. Org. Chem.* **1957**, *22*, 557–558. (b) Batsanov, A. S.; Collings, J. C.; Fairlamb, I. J. S.; Holland, J. P.; Howard, J. A. K.; Lin, Z.; Marder, T. B.; Parsons, A. C.; Ward, R. M.; Zhu, J. *J. Org. Chem.* **2005**, *70*, 703–706.